CROATICA CHEMICA ACTA CCACAA **72** (1) 25–41 (1999)

ISSN-0011-1643
CCA-2558 *Original Scientific Paper*

Structural and Electrochemical Characteristics of Sintered Nickel Electrodes

Eleonora Maria Rus, Delia Maria Constantin, Liviu Oniciu, and Lucretia Ghergari*

Department of Physical Chemistry, Faculty of Chemistry and Chemical Engineering of »Babes-Bolyai« University, 11 Arany Janos, 3400, Cluj-Napoca, Romania (E-mail: norus@chem.ubbcluj.ro)

Received May 28, 1998; revised October 26, 1998; accepted December 7, 1998

Sintered nickel electrodes were prepared from nickel powder obtained by thermolysis of $Ni(NO_3)_2 \cdot 6H_2O$ and by reduction of formed oxides in controlled atmosphere and electrochemical activation in 42% KOH solution. Scanning electron microscopy, X-ray diffraction and cyclic voltammetry were used to investigate the structural and electrochemical characteristics of the prepared electrodes. The diffusion coefficients of the proton in nickel hydroxide were determined. It has been found that the proton diffusion coefficient is higher for the oxidation process in 6 M KOH + 35 g/L LiOH than in 6 M KOH electrolyte. The characteristics and the performance of the prepared sintered nickel electrodes point to the possibility of their successful utilisation as cathodes in alkaline batteries.

INTRODUCTION

The general physico-chemical and electrochemical characteristics of a given cathode material have a great influence on the performance of electrochemical sources.

Nickel hydroxide is a successful cathode material used in Ni-Cd, Ni-Zn, and Ni-Fe alkaline batteries, having a large area of application, and in $Ni\text{-}H_2$ batteries, used extensively in aerospace systems.[1]

* Author to whom correspondence should be addressed.

The reaction at the nickel electrode during charge-discharge is:

$$NiOOH + H_2O + e^- \Leftrightarrow Ni(OH)_2 + HO^- ; \quad \varepsilon^\circ = 0.490 \text{ V/NHE} . \qquad (1)$$

Despite the long technological history of nickel hydroxide electrode, its electrochemistry is not fully understood yet. This is due to the participation of two distinct couples, β-$Ni(OH)_2$ / β-NiOOH and α-$Ni(OH)_2$ / γ-NiOOH, in the potential-determining reactions.[2–5]

Existence of α, β, γ species is related to the method of preparing active material, charge-discharge cycling conditions, and electrolyte concentration and composition.

The best conditions of charge-discharge processes Eq. (1) require easy diffusion of electrolyte inside the electrode. From this point of view, the sintered type electrodes are extremely efficient.[6–8]

Sintered supports are prepared by pressing and sintering the nickel powder on a current collector. Activation is performed by precipitation of active material in the pores of supports by the chemical, electrochemical or thermal method.[9–13]

Formation of electrodes takes place by charge-discharge cycles in controlled conditions. Sintered electrodes have high specific capacities and energies and good mechanical properties.[14,15]

In recent years, much interest has been centred on the development of high energy density nickel electrodes, produced on sintered supports.

In this paper, the results of the structural and electrochemical investigations of the sintered support and nickel electrode prepared by us are presented. The electrochemical properties including charge-discharge characteristics and coulombic efficiency have been investigated by cyclic voltammetry and by voltage-time curves. The proton diffusion coefficients in the nickel hydroxide were calculated using cyclic voltammograms recorded at various potential sweep rates.

EXPERIMENTAL

Sintered nickel supports ($70 \times 35 \times 1$ mm), having *ca.* 70% porosity, were prepared from nickel powder with a diameter <0.1 mm. Nickel powder was obtained by thermolysis of $Ni(NO_3)_2 \cdot 6H_2O$, followed by reduction of the formed Ni_2O_3 and NiO to Ni. Sintered supports were made by pressing a mixture of prepared nickel powder (80%) and $(NH_4)_2CO_3$ (20%) for pores generation on a current collector (a nickel-plated iron screen) and sintering at 800 °C in reduction atmosphere.[16,17]

For activation, the sintered supports, impregnated with nickel nitrate, were anodically polarized between 2 nickel cathodes in 42% KOH solution at a current density of ~30 mA/cm^2. After polarization, the electrodes were washed with distilled water and dried at 80 °C.[18]

The electrochemical behaviour of the prepared electrodes was investigated by cyclic voltammetry in aqueous 6 M KOH solutions with and without LiOH, at room temperature.

The experiments were performed using a Wenking HP 72 potentiostat, a PV2 programmer Meinsberg type, a MV 87 Pracitronic digital millivoltmeter and a NE 230 X-Y recorder. A platinum wire as counterelectrode and a saturated calomel electrode (SCE) as reference were used; all the potentials given in this paper refer to the SCE.

From the charge-discharge curves recorded with a nickel plate counterelectrode, in galvanostatic regime, the coulombic efficiencies of the sintered nickel electrodes were determined.

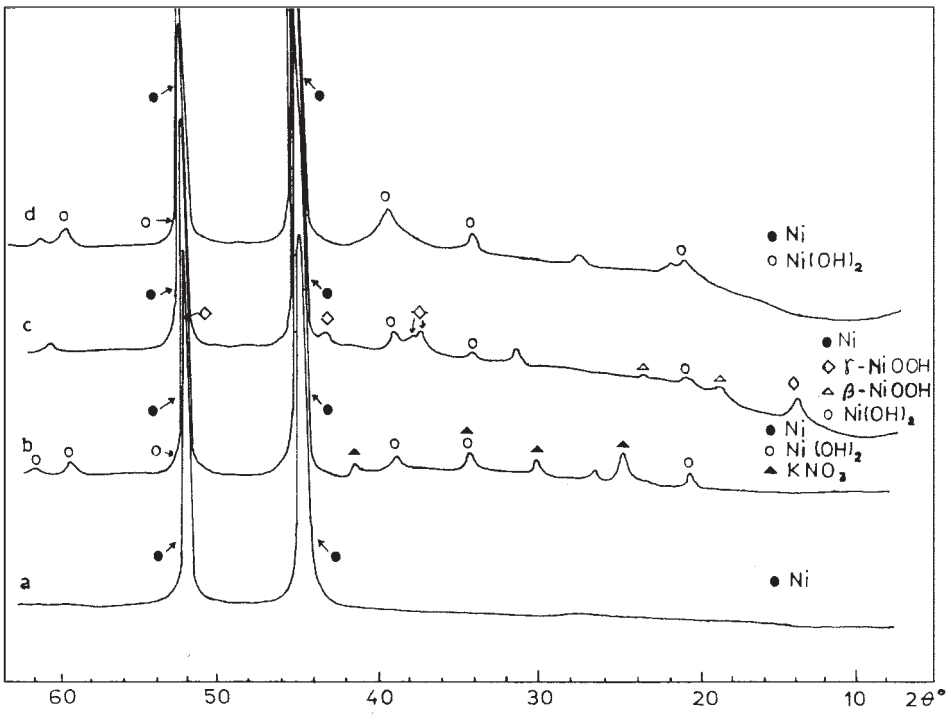

Figure 1. X-ray diffractograms of sintered nickel electrode: a) sintered support, b) uncycled, c) charged, d) discharged.

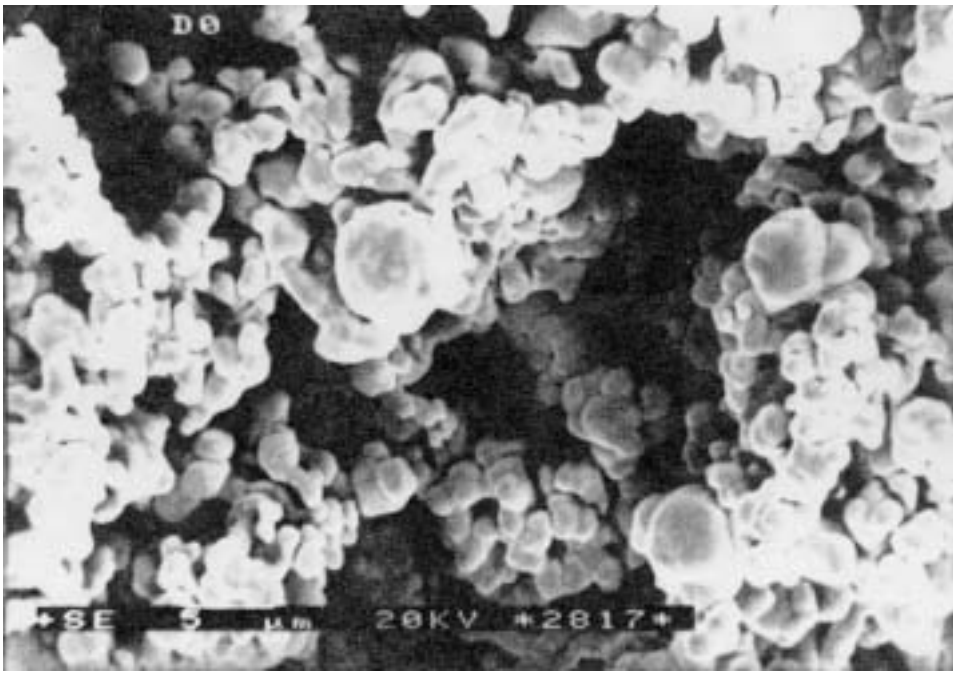

Figure 2. SEM photograph of sintered nickel support.

The crystal morphology as well as the structure of the electrodes was examined by scanning electron microscopy (SEM). Electron micrographs were obtained on a Tesla-Brno BS 340–1990 scanning electron microscope.

Phase compositions of electrodes in different states (uncycled, charged and discharged) were analyzed by X-ray diffraction (XRD) with a DRON–3 type diffractometer with a Cu-cathode, using k_α radiation (λ =1.57051Å).

RESULTS AND DISCUSSION

Study of Sintered Nickel Supports

Structural Characterization

The X-ray diffraction pattern in the 2θ = 4–63° range, obtained on the powder scraped from the nickel support surface, shows two well expressed lines for nickel, (111) and (200) faces (Figure 1, curve a).

Scanning electron microscopic studies show that the sintered support has a microcrystalline structure with porous texture (Figure 2). Nickel crys-

tals, sized between 0.5 and 4 μm, have tabular habitus and form microcrystalline aggregates. Sizes of pores formed between these aggregates are larger than the nickel crystal sizes.

Electrochemical Behaviour

The voltammograms recorded on an inactivated sintered nickel support with an apparent surface area of 1 cm^2 in 6 M KOH at different potential sweep rates are shown in Figure 3.

The potential was scanned between the values at which oxygen evolution reaction (OER) and hydrogen evolution reaction (HER) occurred. Previously, the surface of the electrode was electrochemically treated by cathodic polarization at –1.1 V for 5 minutes. The stabilized form of voltammograms was obtained only after 8 oxidation-reduction cycles.

In the anodic sweep in the region between –1.1 and –0.85 V, the formation of $Ni(OH)_2$ takes place, corresponding to oxidation of a part of nickel particles of the sintered support. Oxidation of $Ni(OH)_2$ to NiOOH and OER takes place at different potential values, depending on the sweep rates [19, 20].

In the cathodic sweep, the reduction of NiOOH to $Ni(OH)_2$ occurs at potentials between 0.090 and 0.130 V, while the reduction of $Ni(OH)_2$ to Ni is not observable because of HER.

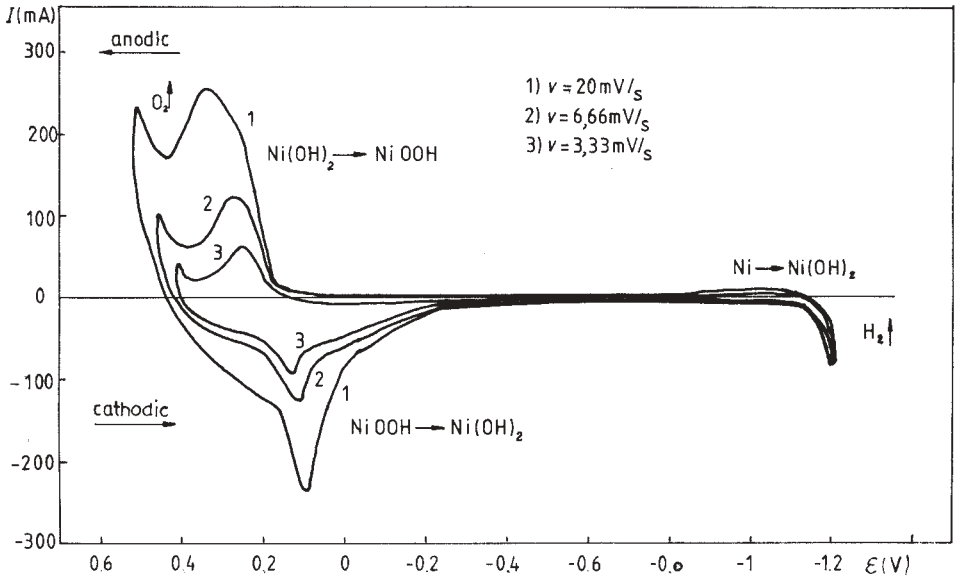

Figure 3. Cyclic voltammograms of sintered nickel support, in 6 M KOH.

The average potential, $\varepsilon' = \frac{\varepsilon_{a,p} + \varepsilon_{c,p}}{2}$, of NiOOH / $Ni(OH)_2$ couple was calculated for all sweep rates (Table I). The determined ε' values are comparable with the theoretical value of reversible potential, ε_r = 0,226 V, in the same solution.[14]

TABLE I

Cyclic voltammetry measurements of the sintered nickel support, in 6 M KOH

v (mV/s)	$\varepsilon_{a,p}$ (V)	$\varepsilon_{c,p}$ (V)	$\Delta\varepsilon_p$ (V)	ε' (V)	$\frac{I_{c,p}}{I_{a,p}}$
20	0.330	0.090	0.240	0.210	0.92
6.66	0.270	0.120	0.150	0.195	1.00
3.33	0.240	0.130	0.110	0.185	1.33

The reversibility of oxidation-reduction processes may be estimated by $\Delta\varepsilon_p = \varepsilon_{a,p} - \varepsilon_{c,p}$ and it gets better as the sweep rates get smaller (Table I). The anodic and cathodic peak currents ($I_{a,p}$ and $I_{c,p}$) are higher as sweep rates increase, probably due to kinetic effects. The $I_{c,p} / I_{a,p}$ ratio increases when the sweep rate decreases.

The higher than unity values of $I_{c,p} / I_{a,p}$ ratio suggest partial transformation of the sintered support in active material. The phenomenon, confirmed by structural investigations (SEM and XRD), explains the utilization coefficients of active material (u), more than 1 obtained in some experimental conditions (see section Electrochemical behaviour).

Study of Activated Sintered Nickel Electrodes

Structural Characterization

The X-ray diffraction pattern in the 2θ = 4–63° range, obtained on the powder scraped from the surface of uncycled nickel electrode, shows well expressed (111) and (200) lines, corresponding to nickel, and some lines of small intensity corresponding to $Ni(OH)_2$ (theofrasit) (Figure 1, curve b).

The electron micrograph of the uncycled electrode reveals a microcrystalline-amorphous structure with porous texture (Figure 4).

The compounds deposited on the support surface have an amorphous aspect, exhibiting irregular fissures of dehydration. The amorphous substance covers the majority of the pores, levelling the previously observed rugosities

Figure 4. SEM photograph of uncycled sintered nickel electrode.

of the support (Figure 2). Large nickel crystals, of cubic, octahedral and mixed cubic-octahedral symmetries can be observed under the amorphous layer. Small nickel crystals disappeared due to their participation in the process of amorphous hydroxide formation.

In the charged nickel electrode, the XRD reveals, besides nickel, appreciable amounts of γ-NiOOH and β-NiOOH (Figure 1, curve c). There is also a smaller amount of $Ni(OH)_2$.

The electron micrograph of the charged electrode shows also a microcrystalline-amorphous structure with porous texture, which has numerous fissures due to dehydration and reorganization of the amorphous film (Figure 5). The reorganization consists of NiOOH formation.

The very small isometric crystals, of 0.5–1 μm, are attributed to γ-NiOOH, whereas the hexagonal crystals of 0.5–3 μm, with tabular and lamellar habitus are attributed to β-NiOOH. Below the microcrystalline film, there is an amorphous substance that covers the sintered support nickel crystals.

The X-ray diffraction pattern in the discharged electrode reveals, besides nickel, appreciable amounts of $Ni(OH)_2$, which represent the discharge active mass (Figure 1, curve d).

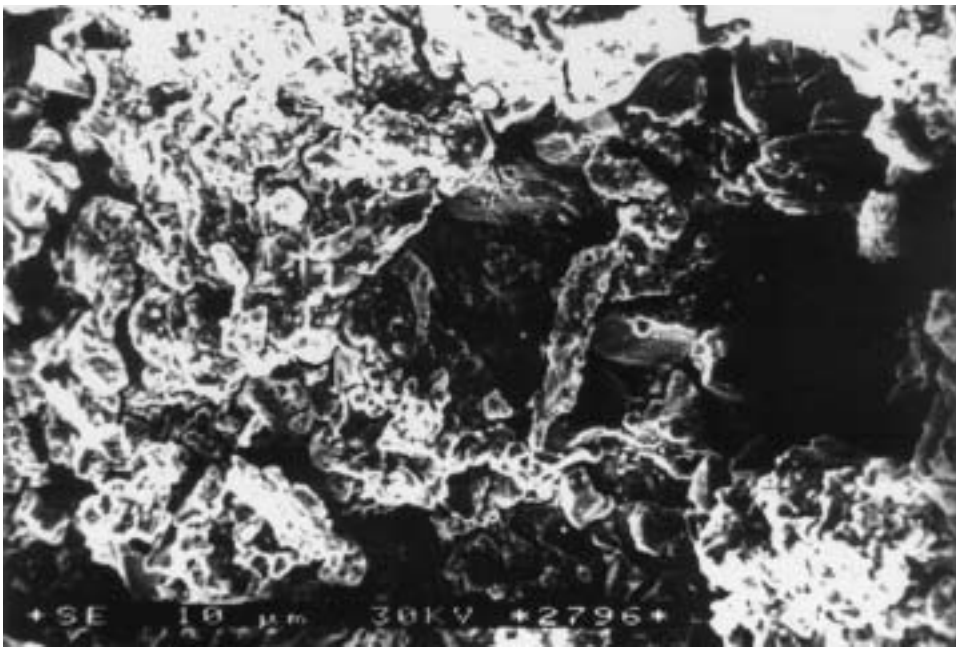

Figure 5. SEM photograph of charged nickel electrode.

Figure 6. SEM photograph of discharged nickel electrode.

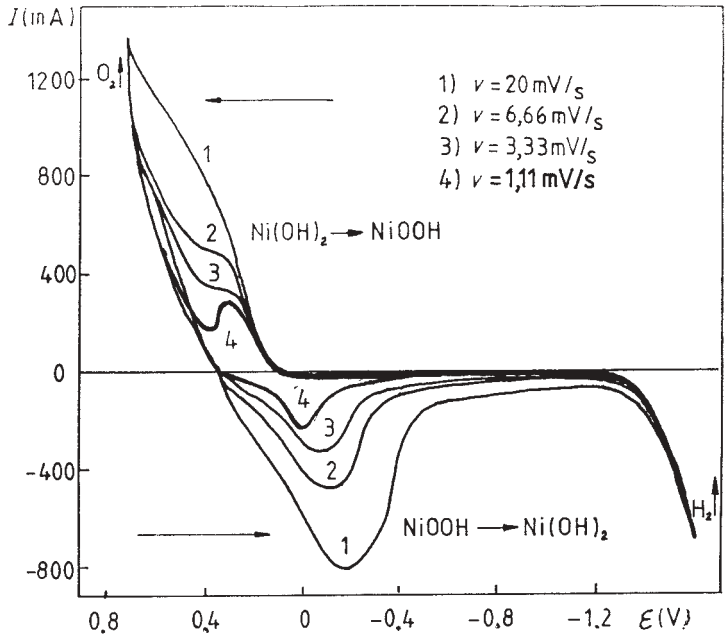

Figure 7. Cyclic voltammograms of sintered nickel electrode in 6 M KOH, at v = 20 (1), 6.66 (2), 3.33 (3), and 1.11 (4) mV/s.

SEM investigation of the discharged electrode shows a porous microcrystalline structure in which two generations of $Ni(OH)_2$ crystals can be distinguished (Figure 6).

The first generation is formed by large (10–25 μm) hexagonal crystals with tabular habitus, on which there are small crystals (0.5–2 μm) in aggregates of rosette form. These crystallites can be observed in the gaps between large crystals. The two different $Ni(OH)_2$ crystals can be attributed to α-$Ni(OH)_2$ and β-$Ni(OH)_2$ having their origin in the two forms of the γ-NiOOH and β-NiOOH charged active mass.

Electrochemical Behaviour

Cyclic voltammetry

Stabilized form of voltammograms for activated sintered nickel electrode was attained after 5 oxidation-reduction cycles, in 0.7–1.4 V range, at v = 20 mV/s (Figure 7). This stabilized profile of voltammograms corresponds to the formatted nickel electrodes of alkaline batteries.

The results of cyclic voltammetry measurements in 6 M KOH are presented in Table II.

TABLE II

Cyclic voltammetry measurements of the sintered nickel electrode, in 6 M KOH.

v (mV/s)	$\varepsilon_{a,p}$ (V)	$\varepsilon_{c,p}$ (V)	$\Delta\varepsilon_p$ (V)	ε' (V)	$\frac{I_{c,p}}{I_{a,p}}$
20	–	–0.180	–	–	–
6.66	0.390	–0.095	0.485	0.148	0.85
3.33	0.375	–0.050	0.425	0.162	0.86
1.11	0.350	0.050	0.300	0.200	0.88

The increased values of $\Delta\varepsilon_p$, in comparison to $\Delta\varepsilon_p$ values of sintered nickel support (see Table I), can be attributed to a more pronounced interference of OER with the active mass charge.

After addition of 35 g/L LiOH in 6 M KOH electrolyte, the stabilized form of voltammograms was obtained in the second cycle after LiOH addition (Figure 8, curve 2), probably after incorporation of LiOH in the active material lattice in the oxidation process.[21–25]

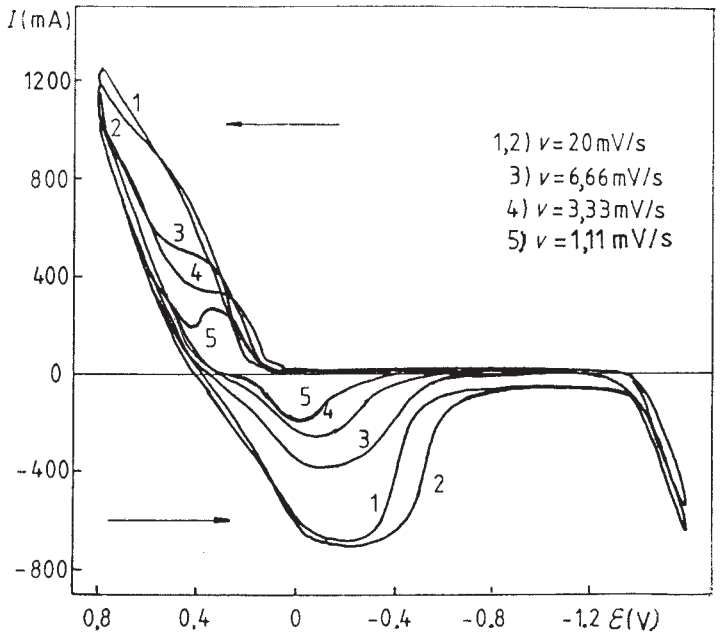

Figure 8. Cyclic voltammograms of sintered nickel electrode in 6 M KOH + 35 g/L LiOH, at v = 20 (1, 2), 6.66 (3), 3.33 (4), and 1.11 (5) mV/s.

Addition of LiOH into 6 M KOH electrolyte determines the shift of average potential ε′ to more anodic values and a slight increase of $I_{c,p} / I_{a,p}$ ratio (Table III).

TABLE III

Cyclic voltammetry measurements of the sintered nickel electrode, in 6 M KOH + 35 g/l LiOH

v (mV/s)	$\varepsilon_{p,a}$ (V)	$\varepsilon_{p,c}$ (V)	$\Delta\varepsilon_p$ (V)	ε' (V)	$\frac{I_{c,p}}{I_{a,p}}$
20	–	–0.220	–	–	–
6.66	0.400	–0.080	0.480	0.160	0.86
3.33	0.380	–0.040	0.420	0.170	0.88
1.11	0.340	0.085	0.255	0.212	0.89

The theoretical and practical discharge capacity values of four electrodes with different amounts of active mass were determined. Theoretical capacity (Q_t) was calculated taking into account the specific capacity of NiOOH (289 mA h/g). Practical discharge ($Q_d = t_d \cdot I_{disch.}$) was determined from discharge measurements in half-cell, in galvanostatic regime ($I_{disch.}$ = 200 mA), at room temperature. The amount of active mass was determined by weigh measurements of unactived and actived electrodes.

The obtained overunity values of the active material utilization coefficient u, (representing the ratio between practical discharge capacity Q_d and theoretical capacity Q_t) can be explained by the participation to the charge-discharge processes of nickel from the sintered support (Table IV).

Linear relationships between the current intensities of the peaks ($I_{a,p}$ and $I_{c,p}$ corresponding to activated sintered nickel electrode voltammograms

TABLE IV

Utilisation coefficients of active material of the sintered nickel electrodes, for $I_{disch.}$ = 200 mA

NR. electrode	Active mass (g)	Q_t (mA h)	t_d (h)	Q_d (mA h)	u
1	2.060	595.34	4	800	1.34
2	2.542	734.63	4.33	866	1.18
3	2.820	814.98	4.66	933	1.14
4	3.120	901.68	4.60	920	1.02

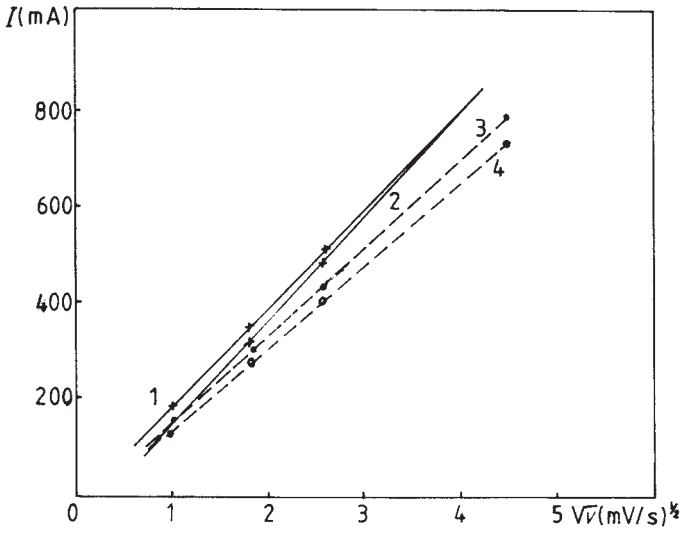

Figure 9. Dependence of the anodic (—), and cathodic (- - -) peak current intensities on $\sqrt{v}$; 6 M KOH (1, 3), and 6 M KOH + 35 g/L LiOH (2, 4).

from Figure 7 and 8) and the square root of sweep rates $\sqrt{v}$ suggest that oxidation-reduction processes that occur are controlled by diffusion (Figure 9).[26]

Accepting that, in the activated sintered nickel electrode, oxidation and reduction processes occur in the solid phase, the charge and the discharge of active material are accompanied by proton diffusion simultaneously with the charge transfer:[4]

$$Ni(OH)_2 \Leftrightarrow NiOOH + H^+ + e^- . \quad (2)$$

Dependence of peak current intensities on the sweep rate is expressed by:[27]

$$I_p = 2.99 \cdot 10^5 \cdot z(\alpha z_a)^{1/2} \cdot A \cdot D_{H^+}{}^{1/2} \cdot c \cdot v^{1/2} \quad (3)$$

where:

I_p = Current intensity of the peak (A);
z_a = Number of electrons, apparently exchanged;
α = Transfer coefficient for z_a electrons;
A = Area of the electrode (cm^2);
D_{H^+} = Diffusion coefficient of proton (cm^2/s);
c = Concentration of active species;
v = Sweep rate (V/s).

From the slopes of the plots $I_p = f(v^{1/2})$, presented in Figure 10, the proton diffusion coefficients can be determined (Table V) using the values: $z = 1$ and $\alpha z_a = 1.5$, indicated in literature for the transformation of $Ni(OH)_2$ to NiOOH.[27]

TABLE V

Proton diffusion coefficient values corresponding to oxidation-reduction processes of the sintered nickel electrode.

Electrolyte	Process	D_{H^+} (cm^2/s)
6 M KOH	oxidation	$4.337 \cdot 10^{-7}$
	reduction	$3.321 \cdot 10^{-7}$
6 M KOH+	oxidation	$4.887 \cdot 10^{-7}$
35 g/L LiOH	reduction	$3.233 \cdot 10^{-7}$

In order to calculate the proton concentration, its equality with $Ni(OH)_2$ concentration was supposed, according to the reaction stoichiometry (2). The concentration of $Ni(OH)_2$ was calculated using the molecular weight $M_{Ni(OH)_2} = 92.7$ and the density $\rho_{Ni(OH)_2} = 25$ g/cm^3.[28]

The obtained D_{H^+} values (Table V) are situated in the range found in literature: $1.10^{-6} - 5.10^{-12}$ cm^2/s.[29–31] The presence of LiOH in electrolyte has a small stimulative effect on the diffusive transport of H^+ in the oxidation processes (Table V). We explain this by the intercalation of Li^+ ions in the $Ni(OH)_2$ lattice, determining the proton mobilization in the crystalline lattice of discharged active material by an ionic exchange process.

Charge-discharge curves

These curves performed in galvanostatic conditions, for $I = 100$ mA, at room temperature, in 6 M KOH, using a nickel plate as counterelectrode and a SCE as reference, are shown in Figure 10.

In charge (Figure 10, curve 1), plateau A corresponds to oxidation of $Ni(OH)_2$ to NiOOH. The increase of potential recorded after about 3 hours of charge shows the beginning of OER. Region B corresponds to the oxidation of active material parallel to OER (overcharge).

Plateau C of the discharge curve (Figure 10, curve 2) corresponds to reduction of NiOOH to $Ni(OH)_2$. The abrupt decrease of the potential, determined by the low conductivity of $Ni(OH)_2$, indicates the end of discharge.[32] Region E is related to HER (overdischarge).

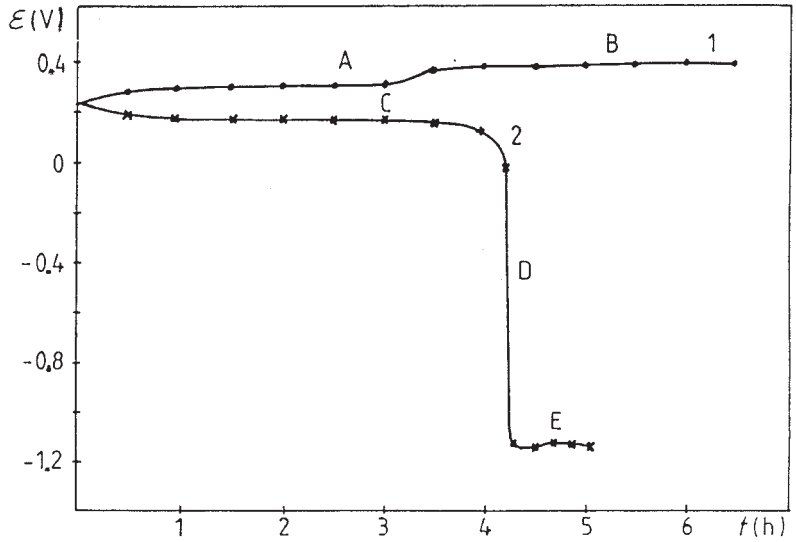

Figure 10. Charge-discharge curves for sintered nickel electrode, in 6 M KOH, at I = 100 mA; 1) charge curve, and 2) discharge curve.

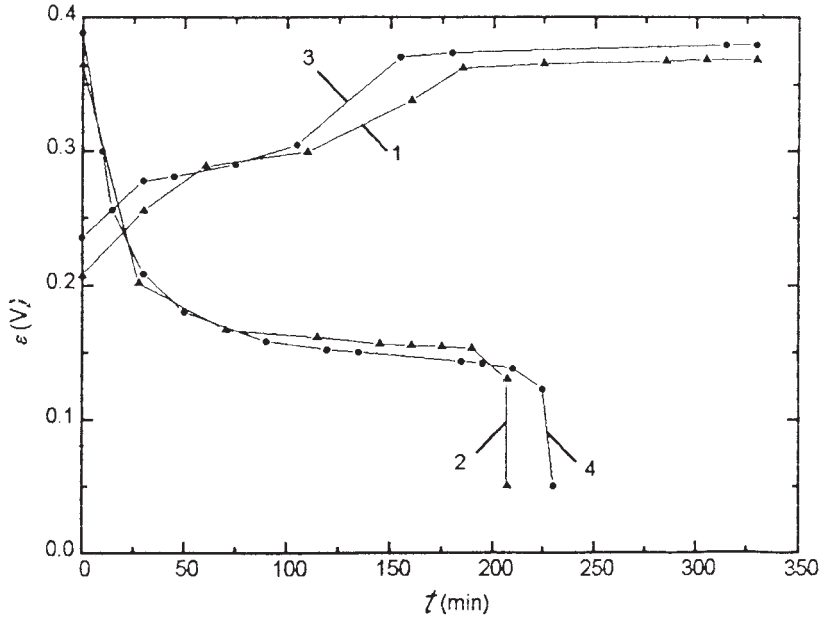

Figure 11. Performance curves for sintered nickel electrode at I = 100 mA in 6 M KOH (1–2), and 6 M KOH + 35 g/L LiOH (3–4).

The coulombic efficiencies, determined from charge-discharge curves plotted in 6 M KOH and 6 M KOH + 35 g/L LiOH, demonstrate the beneficial effect of addition of LiOH into electrolyte (Figure 11 and Table VI). The charge capacity (Q_{charge}) corresponds to charging for 5.5 h at I=100 mA. The discharge capacity ($Q_{discharge}$) was calculated for the time corresponding to the plateau of the discharge curves at I=100 mA).

In the presence of LiOH, the charge potential was higher (Figure 11, curve 3) and the discharge potential was slightly lower (curve 4) than for 6 M KOH electrolyte (curves 1 and 2). However, these effects are counteracted by the increase of the discharge capacity by 10% and that of the coulombic efficiency by 6%.

In was established that the presence of LiOH in electrolyte increases the overpotential of oxygen evolution on nickel (from 0.234 V in 6 M KOH to 0.263 V in 6 M KOH + 35 g/L LiOH), improving the charge efficiency of the electrode.

TABLE VI

Coulombic efficiencies of the sintered nickel electrode

Electrolyte	Q_{charge} (mA h)	$Q_{discharge}$ (mA h)	Coulombic efficiency (%)
6 M KOH	550	350	63.63
6 M KOH + 35 g/L LiOH	550	383	69.64

CONCLUSIONS

From the investigation of structural and electrochemical characteristics of the prepared sintered nickel electrodes, the following conclusions can be drawn:

a) In the charge-discharge cycles, the transformation of some nickel particles of the sintered support in active material takes place. This fact was evidenced by the overunity values of the active material utilization coefficient.

b) The uncycled active material of the sintered nickel electrodes consists, in principle, of $Ni(OH)_2$ in amorphous state.

c) In the charged electrodes, two structural crystalline forms of active material, γ-NiOOH and β-NiOOH, were evidenced.

d) In the discharged electrodes, two forms of $Ni(OH)_2$ crystals, which can be attributed to α-$Ni(OH)_2$ and β-$Ni(OH)_2$, were identified.

e) Addition of 35 g/L LiOH into the 6 M KOH electrolyte enhanced the discharge capacities and the coulombic efficiencies of the prepared sintered nickel electrodes.

f) The characteristics and the performance of our sintered nickel electrodes, prepared by electrochemical activation of sintered supports impregnated with nickel nitrate, point to the possibility of their successful utilization as cathodes in alkaline batteries.

REFERENCES

1. L. Oniciu, E. M. Rus, *Surse electrochimice de putere,* Dacia (Ed.), Cluj-Napoca, Romania, 1978, sect. 7.
2. J. Desilvestre and O. Haas, *J. Electrochem Soc.* **137** (1990) 5c–22c.
3. R. Barnard, C. F. Randell, and F. L. Tye, *J. Appl. Electrochem.* **10** (1980) 109–125.
4. H. Bode, K. Dehmett, and J. Witte, *Electrochim. Acta* **11** (1966) 1079–1087.
5. B. B. Ezhov and O. G. Maladin, *J. Electrochem. Soc.* **138** (1991) 885–889.
6. J. Lomaniec and M. Sokolov, *J. Power Sources* **25** (1989) 159–162.
7. J. Mrha, J. Krejci, Z. Zabransky, V. Koudelca, and J. Malik, *J. Power Sources* **4** (1979) 239–250.
8. R. M. Khalil, *J. Appl. Electrochem.* **18** (1988) 292–297.
9. M. Paszkiewicz, *J. Appl. Electrochem.* **11** (1981) 135–142.
10. B. Lafage, M. Comtat, and R. Routie, *J. Appl. Electrochem.* **18** (1988) 363–367.
11. M. Oshitani, Y. Sasaki, and K. Takashima, *J. Power Sources* **12** (1984) 219–224.
12. M. Wales, *Electrochim. Acta* **24** (1979) 629–631.
13. K. Ho and J. Jorne, *J. Electrochem. Soc.* **137** (1990) 149–158.
14. Delia Maria Constantin, *Ph. D. Thesis,* »Babes-Bolyai« University, Cluj-Napoca, Romania, 1996.
15. L. Oniciu, Eleonora Maria Rus, Delia Constantin, Violeta Voina, and M. Schenker, *Producerea, transportul si utilizarea energiei* **V** (1986) 93–98.
16. L. Oniciu, Eleonora Maria Rus, P. Ilea, Violeta Voina, and Delia Constantin, *Rev. Chim.* **36** (1985) 340–342.
17. L. Oniciu, Delia Constantin, Eleonora Maria Rus, Violeta Voina, and Cristina Corabian, *Studia Univ. »Babes-Bolyai«, Ser. Chem.* **39** (1994) 218–222.
18. L. Oniciu, Eleonora Maria Rus, Delia Constantin, Violeta Voina, and Cristina Corabian, *Producerea, transportul si utilizarea energiei* **XIII** (1994) 161–166.
19. P. V. Kamath and M. F. Ahmed, *J. Appl. Electrochem.* **23** (1993) 225–230.
20. M. J. Avena, M. V. Vazquez, R. E. Carbonio, C. P. De Pauli, and V. A. Macagno, *J. Appl. Electrochem.* **24** (1994) 256–260.
21. R. Barnard, C. F. Randell, and F. L. Tye, *J. Appl. Electrochem.* **11** (1981) 517–523.
22. M. E. Unates, M. E. Folquer, J. R. Vilche, and A. J. Arvia, *J. Electrochem. Soc.* **139** (1992) 2697–2704.
23. O. Lanzi and U. Landau, *J. Electrochem. Soc.* **138** (1991) 2527–2538.
24. S. I. Cordoba-Torresi, C. Gabrielli, A. Hugot-Le Goff, and R. Torresi, *J. Electrochem. Soc.* **138** (1991) 1548–1556.
25. I. P. Gutridge, *US Pat., 3.997.364* (1976).
26. D. M. Mac Arthur, *J. Electrochem. Soc.* **117** (1970) 729–733.

27. C. Zhang and Su-Moon Park, *J. Electrochem. Soc.* **134** (1987) 2966–2973.
28. G. Barral, F. Njanjo-Eyoke, and S. Maximovitch, *Electrochim. Acta* **40** (1995) 709–718.
29. P. de Vidts and R. E. White, *J. Electrochem. Soc.* **142** (1995) 1509–1519.
30. S. Motupally, C. C. Streinz, and J. W. Weidner, *The Electrochemical Society Fall Meeting,* Chicago, Illinois, 8–13 oct. 1995, (Extended abstracts), pp. 64–65.
31. J. Newman, *J. Electrochem. Soc.* **142** (1995) 97–101.
32. M. J. Natan, D. Belanger, M. K. Carpenter, and M. S. Wrighton, *J. Phys. Chem.* **91** (1987) 1834–1841.

SAŽETAK

Strukturna i elektrokemijska svojstva sinteriranih niklovih elektroda

Eleonora Maria Rus, Delia Maria Constantin, Liviu Oniciu i Lucretia Ghergari

Priređene su sinterirane niklove elektrode iz praškastog nikla dobivenoga termolizom $Ni(NO_3)_2 \cdot 6\ H_2O$, redukcijom nastalih oksida u kontroliranoj atmosferi i elektrokemijskom aktivacijom u 42% otopini KOH. Strukturna i elektrokemiska svojstva priređenih elektroda istraživana su elektronskom mikroskopijom, rentgenskom difrakcijom i cikličkom voltammetrijom. Određeni su difuzijski koeficijenti hidrona u krutom niklovom hidroksidu. Utvrđeno je da je koeficijent difuzije hidrona tijekom oksidacije elektrode u elektrolitnoj otopini (6 M KOH + 35 g/L LiOH) veći nego u otopini 6 M KOH. Opisane elektrode mogle bi se koristiti kao katode u alkalnim baterijama.